國立臺灣大學電資學院電機工程研究所

碩士論文

Department of Graduate Institute of Electrical Engineering
College of Electrical Engineering and Computer Science

National Taiwan University

Master thesis

光線追蹤法之平行化加速結構於多核處理器

Parallel KD Tree Acceleration Structures for Ray Tracing on Multi-Core Processor

曾至正

Chih-Cheng Tseng

指導教授：鄭士康 博士

Advisor: Shyh-Kang Jeng, Ph.D.

中華民國 98 年 6 月

June, 2009

致謝

對 3D 動畫技術很嚮往的我，這幾年來每天總要寫程式，也自己念了不少數學。不斷改進遊戲動畫引擎，幾年下來，寫了超過十萬行 C++，也足以自豪。同學們都知道，晚上十點後還有一個人在實驗室寫程式。

這樣的我，卻考進了電機所，爲了畢業，曾經嘗試接觸一些電路、電子、晶片設計的領域，最後還是放棄了。搞了老半天，後來鄭士康老師拉了我一把。回首這段路程，更加清楚自己要的是什麼，幸好，我仍在一條熱血的道路上前進。

我能夠完成這篇論文，最要感謝的是鄭士康老師。鄭老師對學生沒有什麼要求，如果有的話，就是把自己的研究做好。鄭老師處處爲學生著想，卻從來不問學生能幫他什麼，身爲一個資深教授，卻對每個學生都是一視同仁，言出必信，每個學生都很感謝他。在 510 這段期間， 可說是魚與熊掌兼得，不但完成了論文，而且做了許多有意義的事。

印象深刻的是三位開授平行計算的老師，曾于恒老師是流體力學的專家，有時我有數學上的問題，也去請教他；黃乾綱老師對各種程式很有一套，又非常熱心；鄭振牟老師是第一位在台大開授 CUDA，讓人耳目一新。資工所圖學組的三位老師，雖然沒有直接指導過我，但給也過一些不錯的建議。對其他指導過我的師長們，也要說聲謝謝。

感謝實驗室的宗恩、天麟學長，在無形中教了我許多事情。仲耀大、吕大、徐大、SOLO 大、世霖大等同學，都是幽默風趣的強者，再佐以俊嘉、亞聖等搞笑風格，實在覺得這裡不像是實驗室。

也要特別提到動畫工作坊的小鐵、小茶、怡萱、伊寧等，大家一起熬夜做動畫，在我論文交出去的當天，剛好是我們的發表日，太神了！

Abstract

Global illumination is vital in nowadays computer animation, where ray tracing is used to simulate the lighting in real world. Due to the massive computation requirement, the algorithm cannot be applied in real time interactive application. In the era of post Moore’s law, desktop CPU has more and more cores, 8-core and 16-core CPU are going to appear, one can see the prospect of ray traced games.

KD tree is able to fast cull out the empty spaces in the scene, while other structures lack this feature. Especially for unstructured scenes with fast changing geometry where local updates of the structure degrade immediately and a fast reconstruction is preferred.

In the thesis we will skip other parts of ray tracing, but focus on the parallel implementation of the KD tree on multi-core CPU, that is the key to speed up. At beginning we decompose the scene space into sub regions. These sub regions are going to be processed by different cores of CPU. Finally we merge the subtrees into one. We achieve a near fully parallel construction and still preserve a high quality tree.

Keywords: KD tree, global illumination, ray tracing, animation, interactive, game

摘要

全域照明是現今 3D 電腦動畫所必備，其原理在於應用光線追蹤法模擬真實光線，但其計算量極大，故遲遲未能應用在即時性的互動遊戲。在後摩爾定律的年代，桌上處理器核心數量不斷提高，八核及十六核 CPU 不久後將釋出，可以預見全域照明法即將出現在電腦遊戲當中。

在各種加速結構中， KD tree 能夠最有效率的分割場景。特別在沒有關聯性組織的場景中，快速移動的物體，局部性的結構更新很快就失去效力，在這種狀況下通常需要全域性的快速結構重建。

本論文將略過 ray tracing 其他部分，而專注於 KD tree 多核平行化的深入探討，這是加速 ray tracing 的關鍵。將場景分割成許多子空間，再使用多核心 CPU 分別處理分割過的子空間，最後再將子樹合併。我們得到了一個接近完全平行化的建造方法，同時仍然維持著樹的高品質。

關鍵字：全域照明、光線追蹤、電腦動畫、互動、遊戲、空間分割、二元樹

CONTENTS

LISTS OF FIGURES

LIST OF TABLES

Chapter 1 Introduction

1.1 Outline of the Thesis

In the thesis we are going to thoroughly discuss various algorithms of the KD tree. The thesis begins with the fundamentals of ray tracing in Chapter 2. In Chapter 3, the state-of-the-art of KD tree construction is covered. We then present some optimizing techniques in Chapter 4, also the pros and cons of DFS and BFS construction, SOA and AOS node implementation.

Chapter 5 is about how the KD tree construction is mapped to multi-core processor. Highly parallel implementations (the parallel domain partitioning with binning plus the concurrent subtree construction) is addressed. The comparison of 1D binning and 3D binning reveals the trade-off between the construction and traversal of the KD tree.

In Chapter 6 we show that the conventional KD-restart and KD-backtrack can be easily powered with openMP.

The two fundamental operations on GPU are introduced in Chapter 7. The bitonic merge sort and the segmented prefix sum can be used to accelerate the KD tree construction. We also showed the implementations of the two algorithms on CUDA.

1.2 Contributions

For fast KD tree construction, some researchers use three events: starting, ending and lying to classify the triangles. We have proposed a new concept called augmented AABB, where only two events are needed. And we have proved that the augmented AABB is more general, robust and efficient.

We have presented a comparison between the DFS construction and the BFS construction with preallocated memory. And we found that construction with BFS fashion outperform the conventional DFS construction. As far as we know, this comparison is never done before.

For parallel domain partitioning, a prior work resorted to the 1D binning; we have implemented and tested the 3D binning. Although the 1D binning performs faster, for a partition more than 8 the 3D binning makes a good trade-off between the construction time and the traversal time. This observation has never been proposed before.

Chapter 2 Background

2.1 Ray Tracing

Phong's model has dominated the screen of 3D games, where the light source is assumed to be infinitely away from all the objects, and the radiance is merely from the dot product of the surface normal and the light direction.

In physics, photons bounce from surfaces to surfaces, generate reflections and refractions from different materials. If there are obstacles between an object and the light source, the occluded object becomes shadowed, and that is what we want in 3D games. The need for realism stimulates the research of ray tracing.

[33] proposed a simple but powerful model, sometimes called recursive ray tracing. Rays are first shot from virtual camera through each pixel into the scene, they are called "primary rays", and their mission is to find the closest intersection point. And if there is a hit point, a "shadow ray" is launched toward the light source to see if the light is blocked or not. The ray incidence with the geometry surface determines the intensity of radiance, combined with the property of material then we can calculate the shading. Secondary rays are needed to generate the phenomena like reflection or refraction, and

these rays can be spawned recursively, contribute to the shading.

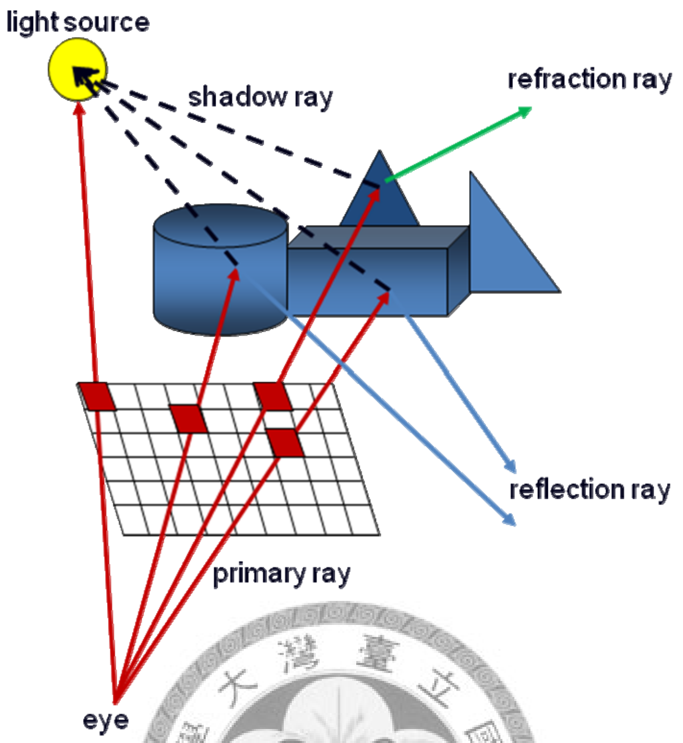

Fig. 2-1 Whitted style recursive ray tracing

2.2 Acceleration Structures

While millions of rays are looking for their nearest collisions in a scene with millions of triangles, it is unlikely to apply a brutal search, instead we resort to some advanced structures. The intersection test of a ray and a triangle is very expensive, and for each ray we cannot afford too many tests, the ability to fast cull away most of the triangles is the most important.

Structures like uniform grid, BVH (bounding volume hierarchy), BSP tree, OBB tree (oriented bounding box), K-Dop, octree, KD tree, have been used in ray tracing.

Chapter 3 Related Work

3.1 Fast KD tree Construction

3.1.1 Introduction

KD tree is a variant of BSP tree, it is widely used in the area of computer graphics and science computing, the relevant applications are not limited to ray tracing, but any problem related to nearest neighbor search. For the scene with few triangles, the construction time can be insignificant compared to the render time. However, modern animations with elaborate scenes and detailed characters usually may have millions of triangles, and the construction time becomes critical.

For earlier GPUs uniform grid was used [21, 22], the structure is simple but fits badly to sparse scenes.

Although structures like BVH can efficiently represent some structured models like characters, where a motion can be handled with local updates of BVH [9], unstructured models like dynamics system make BVH degrade immediately, and a reconstruction from scratch is necessary.

KD tree has been recognized as the best structure for ray tracing [11]. It is able to fast cull away the empty spaces in the scene, which is crucial for wide open scenes where the triangle distribution is sparse. And further, KD tree uses AABB (axis aligned bounding box) as a proxy for geometry primitives, these axis aligned voxels offer extremely fast traversal. Structure like OBB tree [8] is able to fit the primitives well, however the arbitrary orientation make it much slow for traversal.

Variants of KD tree like B-KD tree [29, 34] and SKD tree [12] use two slabs for the split, and simplify the problem of straddling triangles [14]. For such trees left node and right node have overlapped region, and also the two empty spaces at the two ends can be culled. However, they lack an optimized traversal approach like [4, 24, 25]. These trees are not the mainstream and will not be discussed here.

3.1.2 Fast KD tree construction overview

KD tree construction begins as a global voxel which contains the whole scene, called root node, then a top-down fashion binary split is proceeded recursively. Each node is going to split into two children. The pattern continues until the current node no longer has to split, by the time the leaf node usually has only a few triangles.

The process of fast KD tree construction in O(NlogN) can be roughly divided in several stages :

(1) Termination criterion checking

(2) Determine the split axis

(3) Split position evaluation

(4) Classification of triangles

(5) Classification of events

(6) Splice to left and right node

Given a node, we first check some criteria to qualify the node for upcoming stages. If the depth has reached a threshold, or the number of triangles within the node has fallen below a user-specified value, the node then is tagged leaf. Otherwise the node is an internal node.

To split a non leaf node, first we have to choose the split axis. Evaluation of geometry distribution is not trivial and time consuming, the common sense is to always choose the axis with longest extent, or choose in round robin fashion.

3.1.3 Surface Area Heuristic

Split at spatial median is easy, but inefficient. It is important to discard most of the spaces and triangles as early as possible. Our goal is to terminate the ray as fast as we can, and a carefully picked split can make a big difference. The trick is to produce large chunks of empty space close to the root of the tree. [28] has mentioned “Benefits of a good tree are not small”, and may be “several times faster than a mediocre tree”.

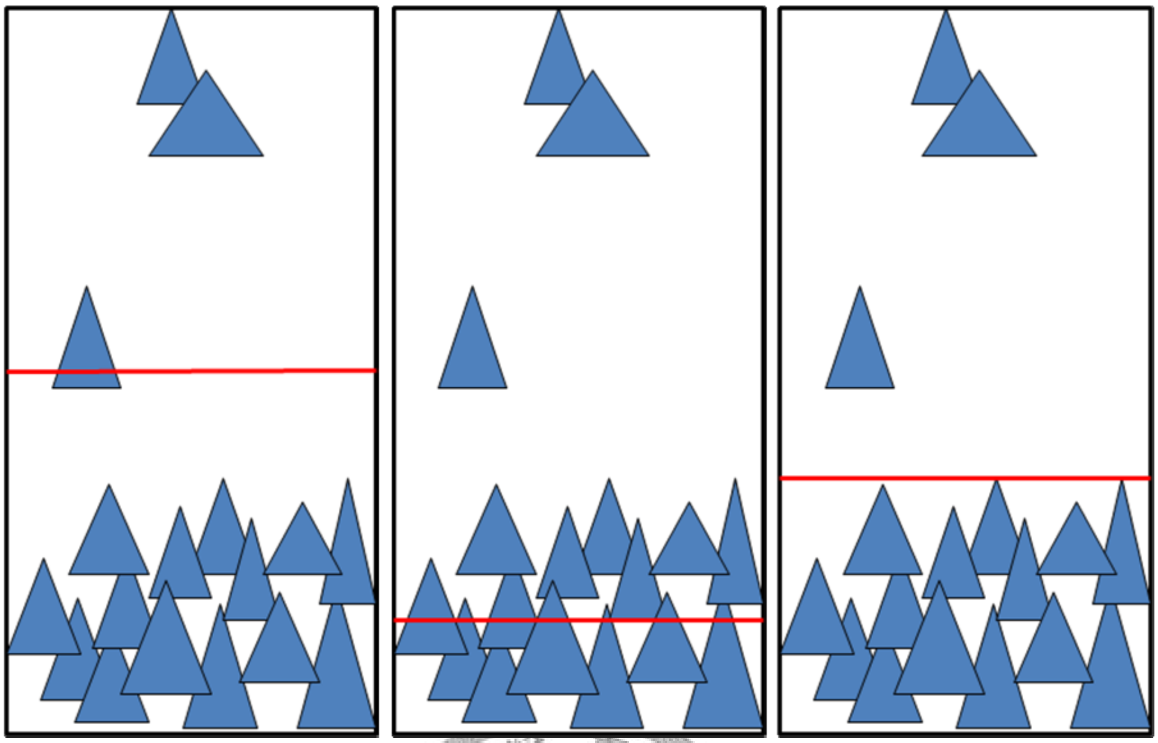

Fig. 3-1 Split at (A) spatial median (B) object median (C) minimum SAH cost

A cost model based on geometric probability of ray has been proposed [11, 15]. The model assumes the rays are uniformly distributed, and the likelihood a ray will intersect the node is roughly proportional to its surface area. Also if the cost of intersection is Ci, the cost of intersection test against N triangles roughly equals NCi.

Based on [15], the cost of tree can be expressed as follows.

C_T:cost of traversal
C_I: cost of intersection test
N_{tri}: number of triangles in the node

$$C = \sum_{All\ nodes} \frac{SA(node)}{SA(root)} C_T + \sum_{All\ leaves} \frac{SA(leaf)}{SA(root)} N_{tri} C_I \quad (3.1)$$

With this cost function, the same triangle may appear in different leaves, and will be tested several times against the same ray. A correct version is derived as follows.

$$C = C_T + C_I\left(\frac{SA(left\ subnode)}{SA(node)}|C_L| + \frac{SA(right\ subnode)}{SA(node)}|C_R|\right) \quad (3.2)$$

Although theoretically CL and CR are going to be recursively evaluated, in fact this approximation works great. The concept is called surface area heuristic, and based on this we can pick the split to minimize the cost of the node.

3.1.4 Split Candidate

Theoretically on the split axis there can be infinite split candidates, nevertheless the cost is piecewise linear along the axis, and it changes only at the AABB planes of the triangle. What we have to consider are these plane positions, also called events of triangle.

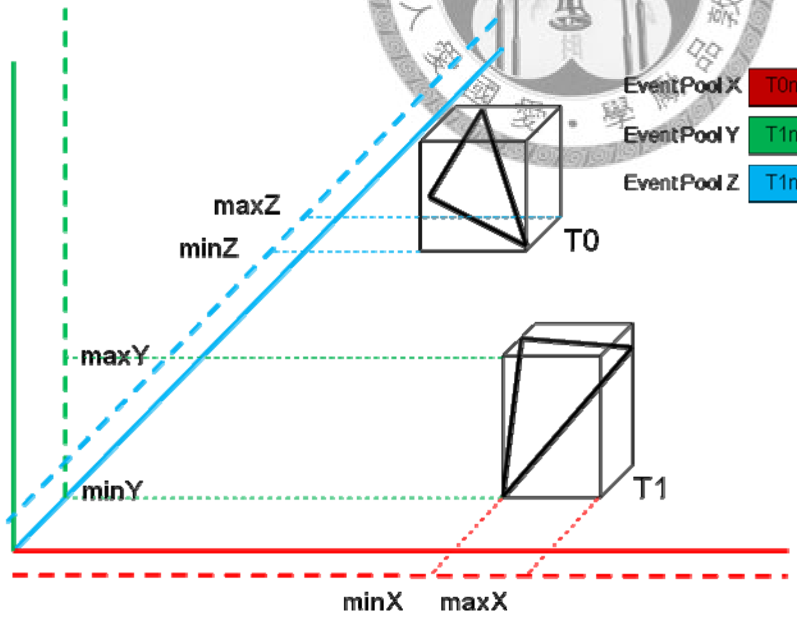

EventPool X	T0min	T0max	T1min	T1max
EventPool Y	T1min	T0min	T0max	T1max
EventPool Z	T1min	T1max	T0min	T0max

Fig. 3-2 Events of triangle

[32] suggested that there are three kinds of event.

$$\begin{array}{l} \text{starting} \Rightarrow \text{min position of triangle on the axis} \\ \text{ending} \Rightarrow \text{max position of triangle on the axis} \\ \text{lying} \Rightarrow \text{min=max if the triangle is perpendicular to the axis} \end{array} \tag{3.3}$$

All events are sorted once at root in ascending order, the order is maintained during the entire construction process. Every node has its own sorted event list, and to each event we perform SAH evaluation. One thing to note is that if we do not maintain the events as sorted, but merely compute the SAH cost for each event individually, then each time we have to count again the triangles to the left and to the right, the complexity is terribly O(N^2).

Taking the advantage of the sorted events, the number of triangles to the left and to the right can be counted incrementally [19, 32]. At the first event, all triangles lie on the right side, so NL is zero and NR has all. By sweeping over the events from left to right, each time we simply increment the NL and decrement the NR, and the cost of all candidates can be known in O(N). Record the event with the minimum cost as the split.

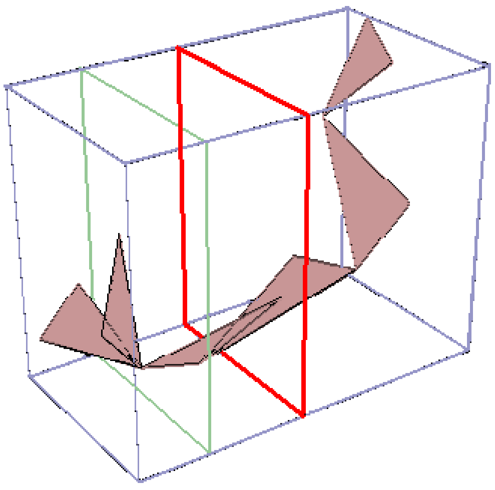

Fig. 3-3 Incremental sweeping for split

p_i^+ : Triangles starting on plane i
p_i^- : Triangles ending on plane i
$p_i^|$: Triangles lying on plane i

```
$N_P^0 = p_0^| \quad N_L^0 = 0 \quad N_R^0 = N - p_0^|$
$for(i = 0; i < numEvents; i++)\{$            (3.4)
    $N_P^i = p_i^|$
    $N_R^i = N_R^{i-1} - p_i^- - p_i^|$
    $\mathrm{cost}_i = SAH(p_i, N_L, N_R)$
    $N_L^i = N_L^{i-1} + p_i^+ + p_i^|$
$\}$
```

A bonus for culling away empty space is suggested [25, 32]. The cost is scaled by about 80% if we choose to split at the position where one side is empty.

Exact SAH evaluation can be approximated by coarsely sampling at finite discrete positions [14]. Especially for nodes near the root this method saves a lot of time without losing much accuracy.

Binning [14, 19, 27] is an alternative to incremental sweeping, the method also has a sort-free like feature, and is able to fast evaluate the cost regardless of the number of triangles. The main problem about binning is the accuracy of the SAH cost, and deeper the node is, more obvious the problem has become. The issues about binning will be discussed later.

3.1.5 Triangle Classification and Clipping

Once the split position has been decided, we are going to distribute the events to left and right. However, some of the events belong to straddling triangles, which contribute its events to both sides, and should be further clipped into two pieces.

So before we process the events directly, we want to tag these triangles as "LEFT", "RIGHT", or "BOTH". An efficient sweeping can be applied as follows.

```
for all t
    side[t]=BOTH;
for all e && $e_{axis}$==splitAxis                                    (3.5)
    if($e_{flag}$== ending && $e_{pos}$<= splitPosition)side[$e_{tri}$]=LEFT;
    else if($e_{flag}$== starting && $e_{pos}$>= splitPosition)side[$e_{tri}$]=RIGHT;
```

Most of the triangles will be marked "LEFT" or "RIGHT", and a few will remain as "BOTH", these triangles straddle the split plane, and need special care.

3.1.6 Event Classification and Generation

There is no problem about dealing with events associated with triangles marked "LEFT" or "RIGHT", these events will be copied to one side with the ascending order unchanged. But for a straddling triangle, its "starting" event lies in left and its "ending" event lies in right. And the triangle should be clipped into two polygons, one for each side.

The precise way is to apply a Sutherland Hodgeman clipping to the triangle, two polygons are generated. We have to calculate the AABB for the two polygons, and replace the old events of the triangle with the new events of the two polygons, on both sides. These new events should be merged with the event arrays to maintain the ascending order.

The process of triangle clipping, with generation of new events and merging of events can be an impact to performance. Fortunately in reasonable cases the number of straddling triangles is minor.

A trivial way is to just copy these events to both sides, and update the events if they exceed the boundaries.

3.1.7 Splice to two children

New memory is dynamically allocated for the two children, or the bias address is incremented if we have preallocated pools.

3.1.8 Termination Criteria

The stages above are performed for each node split, and the ascending order of new event lists are always preserved. The pattern continues until some of the criteria have been achieved.

(1) The number of triangles of the node is smaller than a threshold.

(2) The depth of the node exceeds a threshold.

(3) The split position cannot be found for the node.

The first is mandatory, and the second can be optional. It is notable that we cannot always find a split for every node. In a case where many triangles have the same minimum and maximum on the split axis, the only two split candidates are the minimum and maximum of the node's AABB. The split like this will not be performed, and we either switch to another split axis, or force the node to be a leaf.

3.1.9 Conclusion

All stages required for a node split are presented here.

(1) Termination criteria checking => O(1)
(2) Split axis picking => O(1)
(3) Incremental sweeping for split => O(N) (3.6)
(4) Triangle classification => O(N)
(5) Event classification, generation, and merging => O(N)

Sum up all the stages we get O(N) for one node split. From an easy math the complexity of the whole tree is derived as following.

$$T(N) = N + 2T(N/2) = \ldots \Rightarrow O(N\log N) \tag{3.7}$$

This is the fastest we can get for KD tree construction so far. However, for interactive games with millions of triangles even the best optimized algorithm is not enough, and we have to look for help from hardware.

3.2 Parallel KD tree Construction on Multi-Core CPU

3.2.1 Introduction

[27, 32] have demonstrated KD tree construction on multi-core CPU. They have proposed the method to partition the scene domain into sub-regions, and build sub-trees in parallel. [32] has done the domain partitioning in serial, and the scalability is sub-linear with the number of processors. [27] has proposed a fully parallel implementation with initial clustering based on binning, and achieved good scalability.

3.2.2 Binning

[19, 27] advocate the sort-free sweeping, but improve the performance by applying coarser sampling, also called binning. Binning is similar to pigeonhole and bucket sorting, which is originally devised for points. For triangles, the conventional binning is improper for SAH evaluation, and a min-max binning is used instead [27].

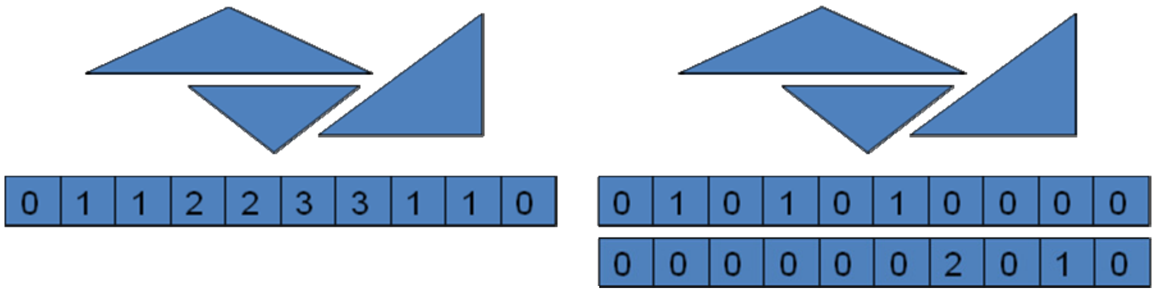

Fig. 3-4 Conventional binning and min-max binning on one axis

3.2.3 Initial Clustering

There are two ways to construct the tree. First, all threads work together to build the whole tree, the problem is that everyone needs to access all the primitives, this demands large cache of all the processors and usually causes race condition. A better way is to evenly divide the tree into subtrees, and each subtree is handled by exactly one thread. This makes sense since subtrees can be stored in the local memory of the processor in charge. Therefore each processor has its own primitive pools to work on, and the memory traffics are reduced.

[19] used only one thread to do the initial partitioning task, and [27] proposed an initial clustering in parallel. They first uniformly distribute all primitives to all processors, and all threads run the binning on their portion of primitives. And by splitting at object median they evenly divide the bins of the selected dimension into segments, and then each segment of the bins is assigned to one thread. Now all the threads know its own set of primitives, and subtrees are built in parallel.

Chapter 4 Optimizing KD tree Construction

4.1 Augmented AABB

We have made some modifications to the fast KD tree construction [32]. They mentioned that three kinds of event are used: “starting”, “ending” and “lying”, triangles lying in the split plane should be placed into either left or right, depends on SAH evaluation [32]. However, from our experiments we observed that additional conditions are needed for “lying” events, and these conditions complicated the process.

We do not see the benefits from using “lying” events; instead we advocate the method using minimum and maximum of the AABBs [19]. This is also more general and robust, since KD tree is not always for triangles; any primitive can be an element of KD tree and can be easily fit into an AABB.

Based on our observation, benefits are induced if we use the min-max events of the AABBs.

(1) Only one bit flag is required to tell from minimum or maximum.

(2) The number of events is automatically double the number of triangles, on all three axes.

(3) Simplify the incremental sweeping.

(4) Simplify the SAH cost function; eliminate the situation that some triangles lie on the split candidate.

(5) Simplify the classification of triangles and events.

(6) Simplify the condition branch in ray traversal.

Based upon our observation at least 10% speedup is achieved. Unfortunately some problems arise from the modification. The incremental sweeping for SAH now becomes as follows.

```
$N_L^0 = 0 \quad N_R^0 = N$
$for(i = 0; i < numEvents; i++)\{$
    $N_R^i = N_R^{i-1} - p_i^-$
    $\mathrm{cost_i} = SAH(p_i, N_L, N_R)$                (4.1)
    $N_L^i = N_L^{i-1} + p_i^+$
$\}$
```

Triangles lying on the plane orthogonal to the split axis generate minimum and maximum of the same value. You can see that such triangles are omitted by SAH function, since by the time the triangles have already been deleted from NR, but have not been added to NL. Let us see the case below.

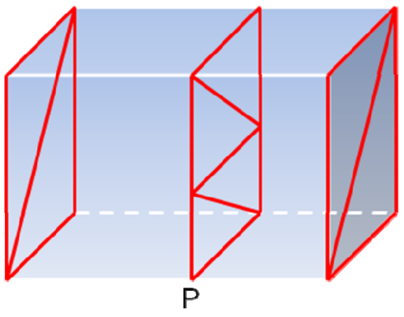

Fig. 4-1 At the time the sweeping reaches the plane p, we have NL = 2 and NR = 2

A remedy to this is to augment the AABB; we decrease the minimum and increase the maximum by an epsilon. Now the SAH function works correctly.

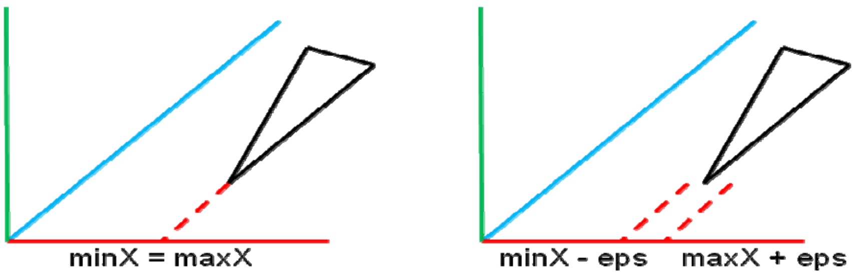

Fig. 4-2 Augmented min-max events of the AABB

4.2 A Trivial and General Method for Event Classification

The standard event classification for straddling triangles [32] requires Sutherland Hodgeman clipping and merging of the new events with the originals. The approach seriously complicates the event classification, and cannot be applied when primitives other than triangle are used. Here we use a general and robust method to handle the straddling AABBs. The pseudo algorithm is as follows.

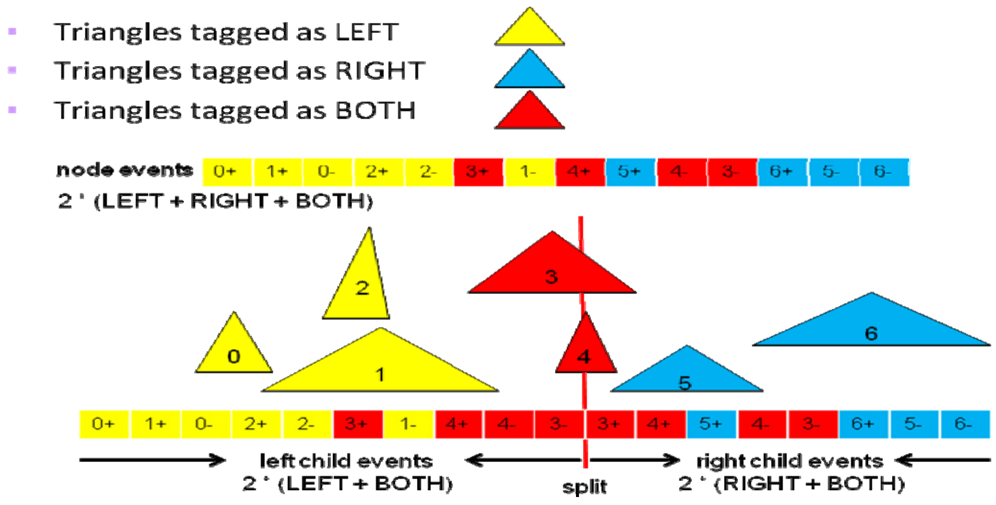

Fig. 4-3 A trivial and general method for event classification

```
for all e on the splitAxis S0
   if(side[e] == LEFT)
      Event_L[S0][numE_L[S0]++] = Event[S0][e];
   if(side[e] == RIGHT)
      Event_R[S0][numE_B[S0]/2 + numE_R[S0]++] = Event[S0][e];
   if(side[e] == BOTH)
      if(Event[S0][e] is ending)
         Event_L[S0][numE_L[S0] + numTriBOTH + numE_BL[S0]++] = Event[S0][e];
         Set the event position as splitPosition
         Event_R[S0][numTriBOTH + numE_R[S0]++] = Event[S0][e];
      if(Event[S0][e] is starting)
         Event_L[S0][numE_L[S0]++] = Event[S0][e];
         Event_R[S0][numE_BR[S0]++] = Event[S0][e];
         Set the event position as splitPosition

for all e on the non-splitAxis S=(S0+1)%3 and S=(S0+2)%3
   if(side[e] == LEFT)
      Event_L[S][numE_L[S]++] = Event[S][e];
   if(side[e] == RIGHT)
      Event_R[S][numE_R[S]++] = Event[S][e];
   if(side[e] == BOTH)
      Event_L[S][numE_L[S]++] = Event[S][e];
      Event_R[S][numE_R[S]++] = Event[S][e];
```
(4.2)

This method works excellently in the situation where most of the primitives have similar sizes. And further, this method helps us handle non-triangle based surfaces.

4.3 Using Preallocated Pools

A major bottleneck of KD tree construction is the rapid memory allocation. [2, 27] have proposed the concept of pre-allocated pool, and we have used a similar method.

The difficulties arise from the prediction of the final size of the pools. The method to precisely estimate the size of nodes and leaves of the whole tree remains unknown. [27] has used chunks of memory linked into lists for nodes and leaves. They perform the construction in DFS fashion, and if the current chunk is full they allocate a new one.

Similarly we deploy one node pool and one leaf pool. At each level we first check if the remaining space is enough for the next level. If necessary we allocate a larger pool and move over the original arrays.

Based upon our experiments, the construction with preallocated pools is at least twice faster than the one using dynamic allocation.

4.4 DFS KD Tree Construction with Preallocated Pools

KD tree is generally constructed in DFS. [27] proposed a DFS construction with preallocated memory, here we present a similar implementation.

The node pool and leaf pool grow constantly during construction. Merely two temporary arrays are needed, array A for left sub-nodes and array B for right sub-nodes. As one node splits into two, we replace the events of the node with the events of its left child in array A, and the events of its right child are "pushed" to array B. Array B actually serves like a stack, each time the split reaches a leaf, the events of the newest node in array B are "popped" to array A. Node split always takes place in array A.

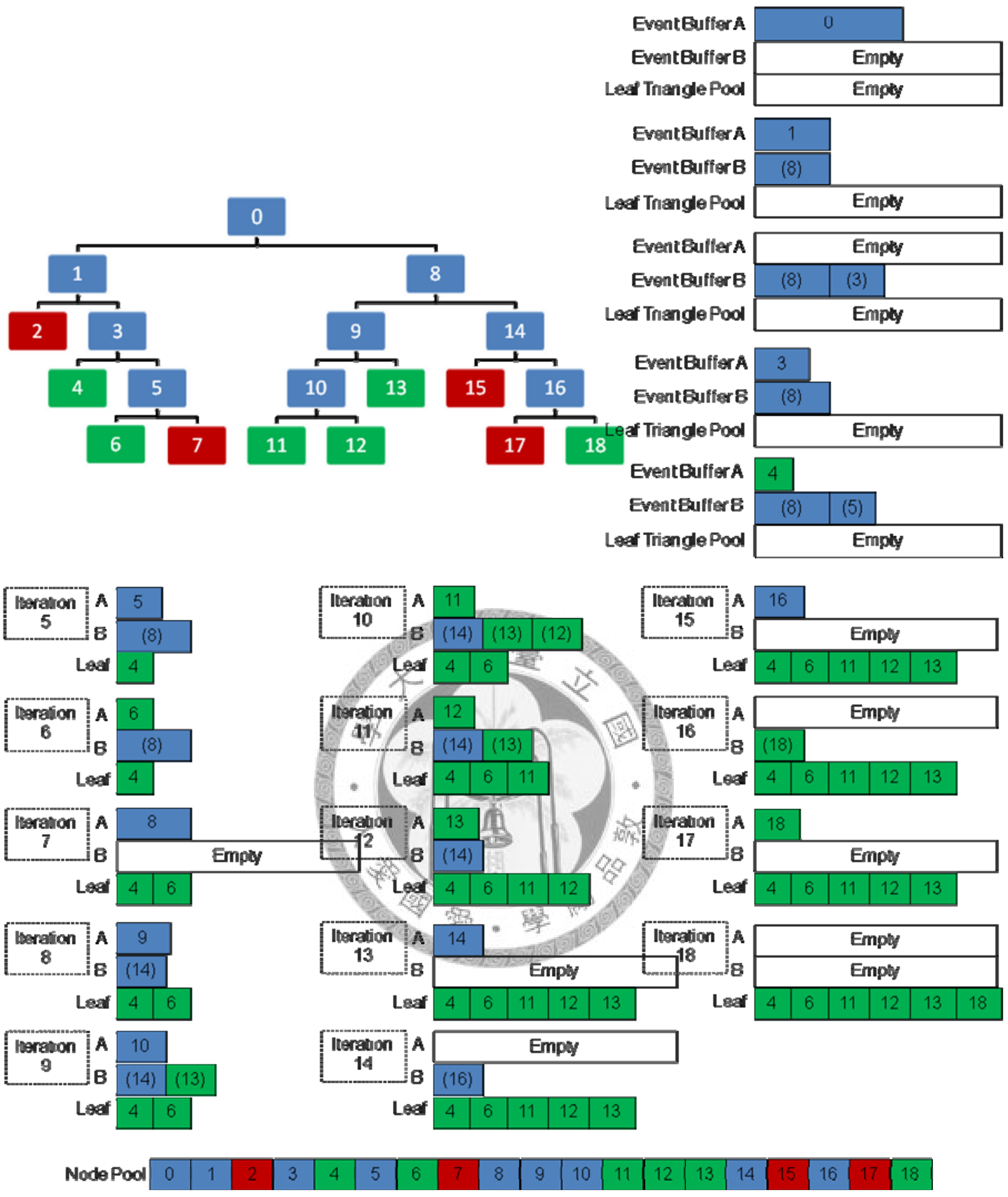

Event Buffer A 0
Event Buffer B Empty
Leaf Triangle Pool Empty
Event Buffer A 1
Event Buffer B (8)
Leaf Triangle Pool Empty
Event Buffer A Empty
Event Buffer B (8) (3)
Leaf Triangle Pool Empty
Event Buffer A 3
Event Buffer B (8)
Leaf Triangle Pool Empty
Event Buffer A 4
Event Buffer B (8) (5)
Leaf Triangle Pool Empty
0
1
8
2
3
9
14
4
5
10
13
15
16
6
7
11
12
17
18
Iteration 5 A 5 B (8) Leaf 4
Iteration 6 A 6 B (8) Leaf 4
Iteration 7 A 8 B Empty Leaf 4 6
Iteration 8 A 9 B (14) Leaf 4 6
Iteration 9 A 10 B (14) (13) Leaf 4 6
Iteration 10 A 11 B (14) (13) (12) Leaf 4 6
Iteration 11 A 12 B (14) (13) Leaf 4 6 11
Iteration 12 A 13 B (14) Leaf 4 6 11 12
Iteration 13 A 14 B Empty Leaf 4 6 11 12 13
Iteration 14 A Empty B (16) Leaf 4 6 11 12 13
Iteration 15 A 16 B Empty Leaf 4 6 11 12 13
Iteration 16 A Empty B (18) Leaf 4 6 11 12 13
Iteration 17 A 18 B Empty Leaf 4 6 11 12 13
Iteration 18 A Empty B Empty Leaf 4 6 11 12 13 18
Node Pool 0 1 2 3 4 5 6 7 8 9 10 11 12 13 14 15 16 17 18

Fig. 4-4 DFS KD tree construction (Blue for internal, green for leaf, red for empty), IDs in brackets are undefined

Note that while the nodes reside in the stack (array B), their node ID are still undetermined. The node is assigned an ID and added to the node pool only after it is popped to array A.

4.5 BFS KD Tree Construction with Preallocated Pools

We perform the construction in BFS style, each time we process one level of the tree. The same two temporary arrays are needed. All the nodes of the first level reside in array A. After we perform the split all the children are moved to array B. And next time array A becomes the input. The two arrays are used alternately until the maximum level is reached.

Any node generated is moved to the node pool, and its bias address in the pool will be record as the left or right child of its parent node. Also any node detected as leaf will have its events moved to the leaf pool.

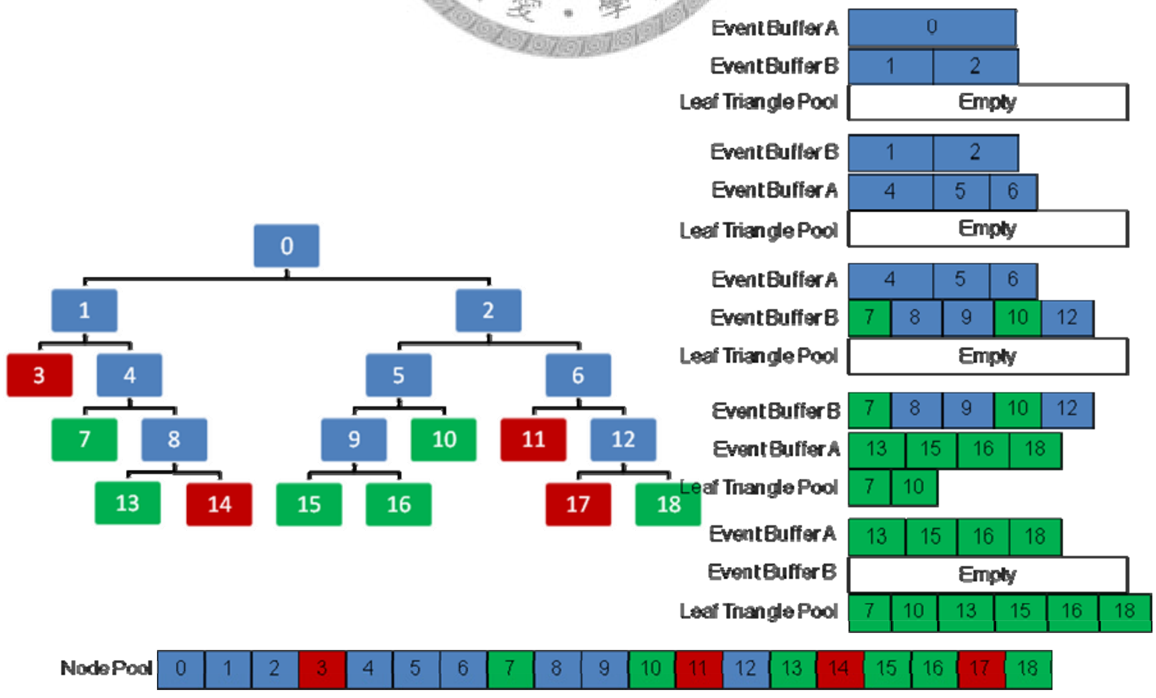

Fig. 4-5 BFS KD tree construction (Blue for internal, green for leaf, red for empty)

4.6 KD Tree Construction: DFS VS BFS

The DFS fashion benefits from always choosing the left child to split, and there is no need to store the AABB min/max. Therefore it consumes less memory than the BFS fashion.

At traversal stage, DFS has another advantage of always placing the left child immediately after the node in the node pool. This increases the data coherent and may perform better when the cache size is small. The fashion is necessary for efficient traversal [13, 20].

The BFS construction demands many fewer iterations, only one iteration for one level. On the other hand, DFS suffers from rapid stack operations, each time a node is split, the right child has to be pushed to array B; and each time the split reaches a leaf, one node in array B has to be popped to array A. The frequent memory traffic considerably limits the performance.

Based upon our experiments, construction using BFS is about 25% faster than that using DFS. Thus we have adopted BFS as our default throughout all the upcoming chapters.

4.7 KD Tree Node Structures: AOS VS SOA

Although storing nodes as array of structures (AOS) may be more straightforward, structure of arrays (SOA) is necessary for parallel implementations. Especially for some architecture like NVIDIA CUDA, where structure and class are not supported and SOA must be used.

For traversal as KD-restart rather than KD-backtrack, the AABB min/max can be omitted, as well as the pointer to parent.

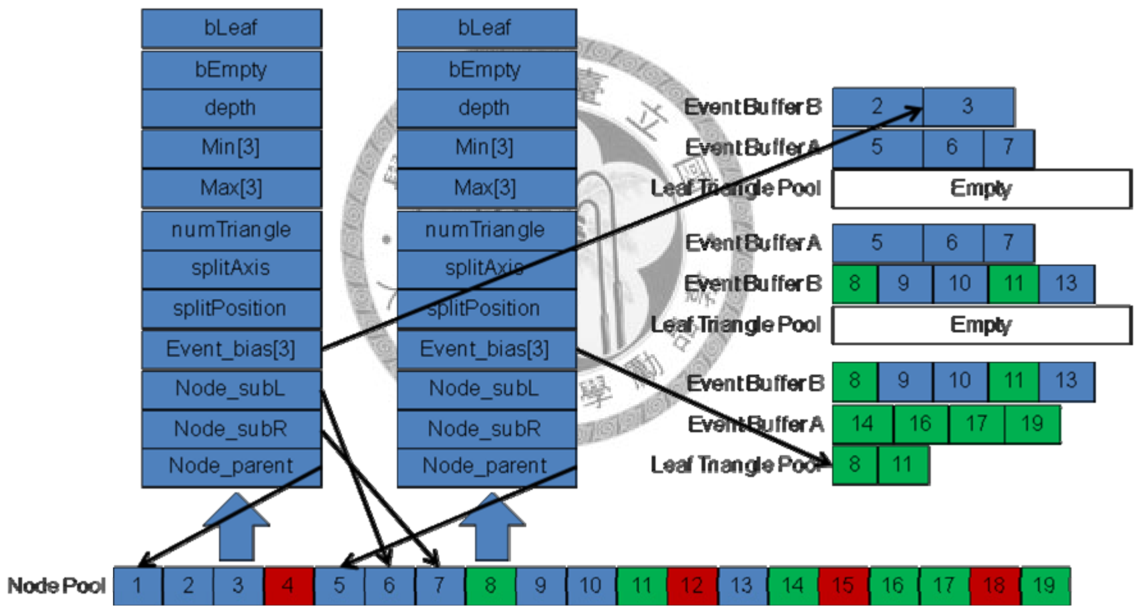

Fig. 4-6 BFS construction with node pool implemented as array of structure (AOS)

Chapter 5 Parallel Construction on Multi-Core CPU

5.1 OpenMP Standard

Nowadays there are two major parallel programming models; one is openMP [6], based on shared memory architecture, the other is MPI [23], or the message passing interface. OpenMP has a huge advantage of keeping the sequential and parallel codes identical. Directives are used to tell the compiler whether to parallel the region or not, this preserves the original sequential codes. OpenMP is also portable; the codes can be ported to various machines without modification. Here we choose openMP as our parallel implementation.

5.2 Domain Partitioning in Serial

Our goal is to divide the scene into disjoint regions with roughly the same number of primitives, and each region represents a subtree. Simply divide at primitive median and we can have two sub-domains with roughly equal primitives.

At first one thread is in charge of the construction, the only difference is that we simply use the event median rather than incremental sweeping SAH for the split position. The construction is proceeded until a certain level, where each node of the level will be the root of a subtree at the next stage. For example, if we need eight subtrees, the construction is performed until level three is done.

The events of these nodes are moved to the event arrays of the subtrees.

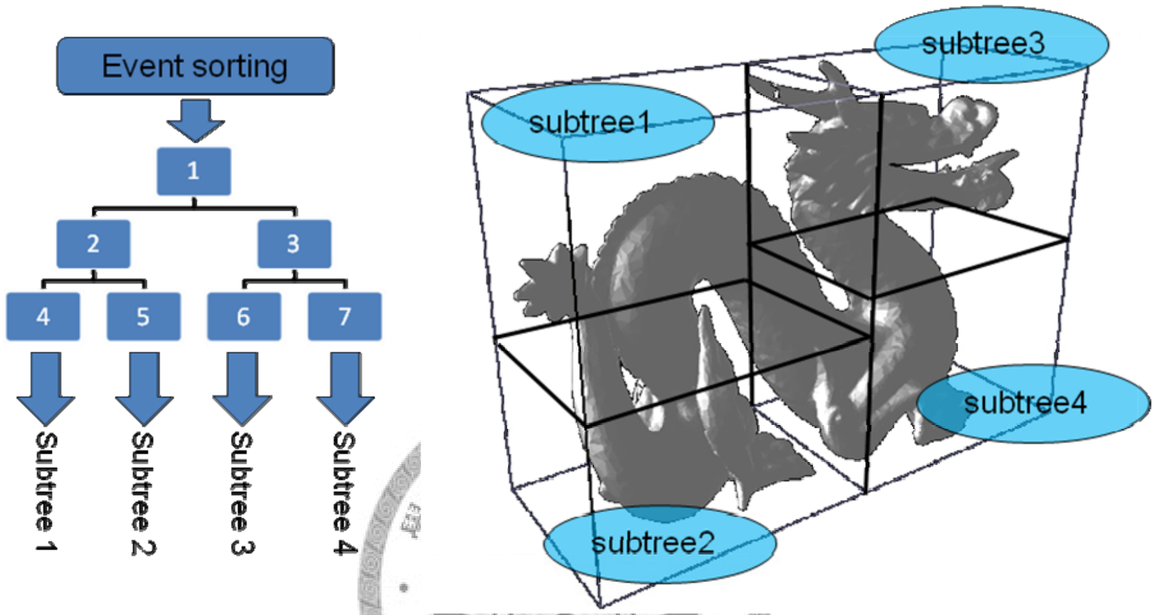

Fig. 5-1 Domain partitioning in serial

5.3 Subtree Construction in Parallel

Let each subtree have its own node pool and event pool; we assign them to threads and run the subtree construction in parallel.

$$\begin{aligned}&\#\text{pragma omp parallel for}\\&for(\text{int } sub = 0;\, sub < numSubtree;\, sub++)\\&\quad buildSubTree(sub);\end{aligned} \tag{5.1}$$

According to the number “sub” it has been assigned, each thread knows which pools to work on.

The subtree construction is totally the same as the regular construction we have mentioned in the previous chapter.

5.4 Merging of Subtrees

After the subtree construction is done, every subtree has its own node pool and leaf pool. As we would hope to maintain the same ray traversal codes, we must merge the sub-arrays into a whole one.

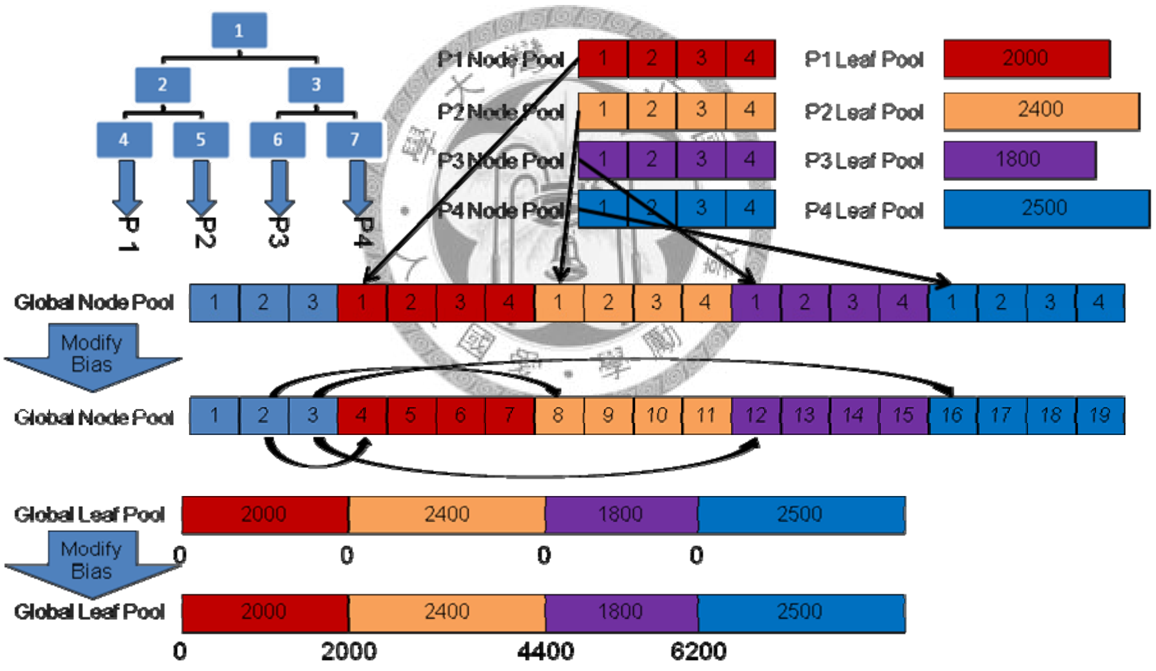

Fig. 5-2 Merging of sub-arrays

5.5 Event Sorting on GPU

Since all events are sorted at root only once, and the ascending order is maintained during the overall construction, much time can be saved if we can do the sorting in parallel. For a model with 60k triangles, there are 120k events on all three axes, thus we have to do a sorting of 120k elements 3 times. We use a bitonic merge sort on GPU for the sorting; the details are discussed in Chapter 6.

Although GPUs afford extreme performance for the root event sorting, the domain partition here is still performed in serial. Also it is unlikely to expect that every desktop has a decent GPU card, let alone a laptop. The implementation differs from various GPUs, and we know that NVIDIA is not the sole vendor in the market.

5.6 Domain Partitioning in Parallel Using 1D Binning

To achieve a higher scalability we must do the initial partitioning in parallel as well. By intuition we would like to do the event classification in parallel, but this is not going to work out. Multiple threads work together on the same event lists, this cause race condition. Of course we can evenly distribute the events to threads, but in order to maintain the ascending order additional merge sorts are inevitable.

Rather than partitioning the sorted events, we instead partition the triangles. We pigeonhole all the triangles on one selected axis, this is called binning [27]. And by accumulating the triangles one can decide at which bin the region is split. Finally we will have regions with roughly equal number of triangles.

First we calculate the minimum and maximum of the whole scene on the three axes, and find the axis with the longest extent to perform binning, this can be done in O(N). A fixed number of bins are set on the selected axis. All triangles are evenly distributed to threads, and all threads perform the min-max binning in parallel. And then we increment one bin at a time to accumulate the triangles from the minimum to the maximum, if the accumulated triangles are larger than the percentage (25% if 4 sub regions), we mark the left boundary of the bin as one boundary of the sub region.

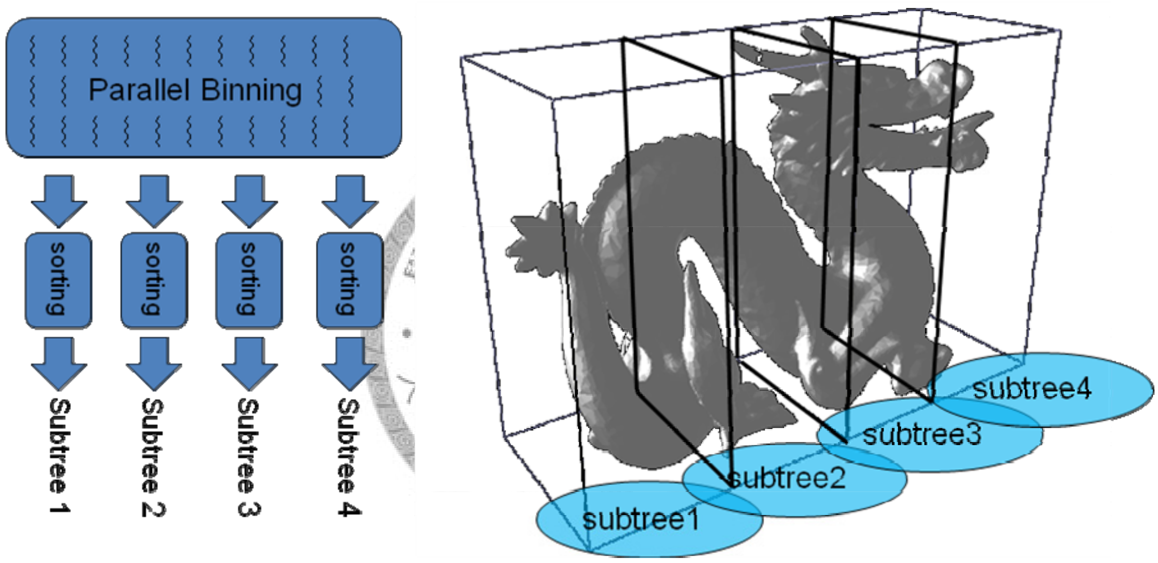

Fig. 5-3 Parallel 1D binning for domain partitioning

After all boundaries of the sub regions have been decided, we classify all triangles into sub regions, also in parallel. Now all subtrees have roughly the same number of triangles, and by sorting each subtree has its own sorted event list.

Not only are the triangles binned in parallel, but also the event sorting is done in parallel. The scalability has improved drastically.

5.7 Domain Partitioning in Parallel Using 3D Binning

Binning on one dimension is easy, but may finally reach a "tipping point". For a partition of 8, 16 and up, the space becomes "slices of bread". The quality of tree degrades seriously, and we can see that the performance of ray traversal plunges.

A remedy to this is to perform the binning on all three dimensions. However, another difficult arises as that we cannot bin all the triangles into its sub-region at one step. Therefore the binning is factored into DFS or BFS fashion.

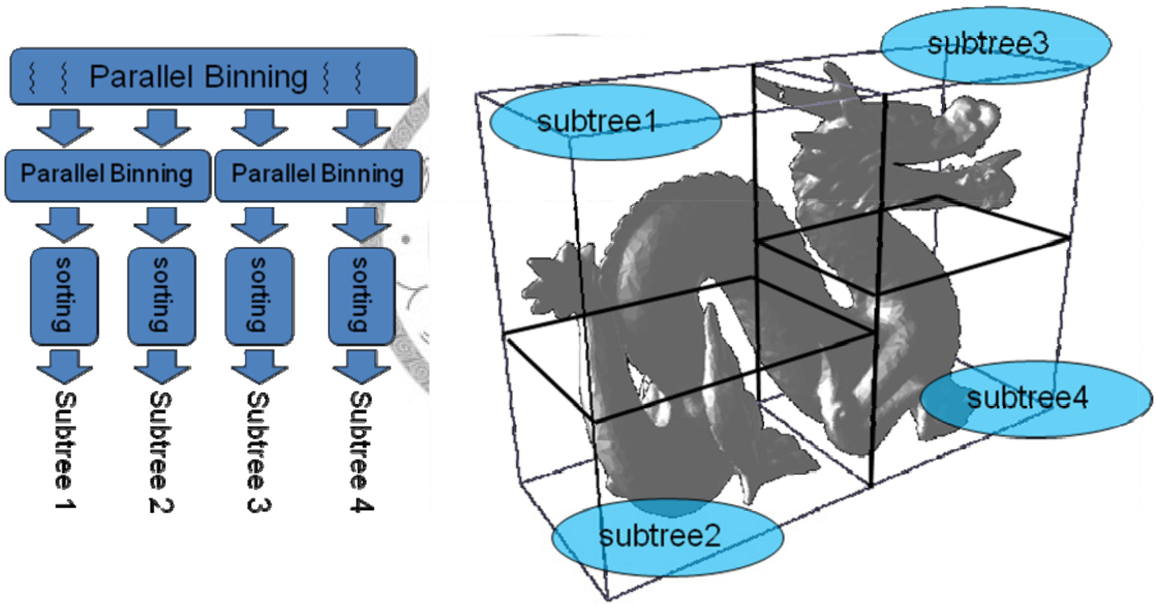

Fig. 5-4 Parallel 3D binning for domain partitioning

The 3D binning is slower, but better preserves the quality of tree. For a partition fewer than 8 we still prefer 1D binning.

Chapter 6 Single Ray Traversal on Multi-Core CPU

6.1 The Standard Traversal

Given a constructed tree, every ray starts at the root, and goes down for a hit. According to the split plane of the current node, the ray may intersect with only left or right child, or both. If the ray intersects only with the left child, we can easily advance the ray to the left child. A ray straddles the split slab must have intersections with both children, by the direction sign on the split axis, either left or right will be traversed first, and the other child will be pushed onto the stack. The pattern is repeated until the ray has reached a leaf, and if the ray finds no hit in the leaf, one node will be popped from the stack, where the down traversal starts again. This is the standard approach [18], on the stack one node is closer to the ray origin than all nodes behind it.

6.2 The Stackless Traversal

The standard approach demands one stack per ray. Since for GPU the cores process many rays simultaneously, and the shared memory among cores usually is limited, the per ray stack approach becomes problematic. [7] presented two stackless traversal methods, called KD-restart and KD-backtrack.

A segment of ray can be represented as a time interval [t_min, t_max]. At beginning we have the entire range, and during the down traversal the interval [t_min, t_max] keeps being modified until we reach a leaf. If there is no collision found in the leaf and the ray has not reached its end, instead of popping a node from the stack we merely advance the segment. At the time the new t_min is assigned the value of t_max, and the traversal either restart from the root (KD-restart), or from the closest ancestor (KD-backtrack).

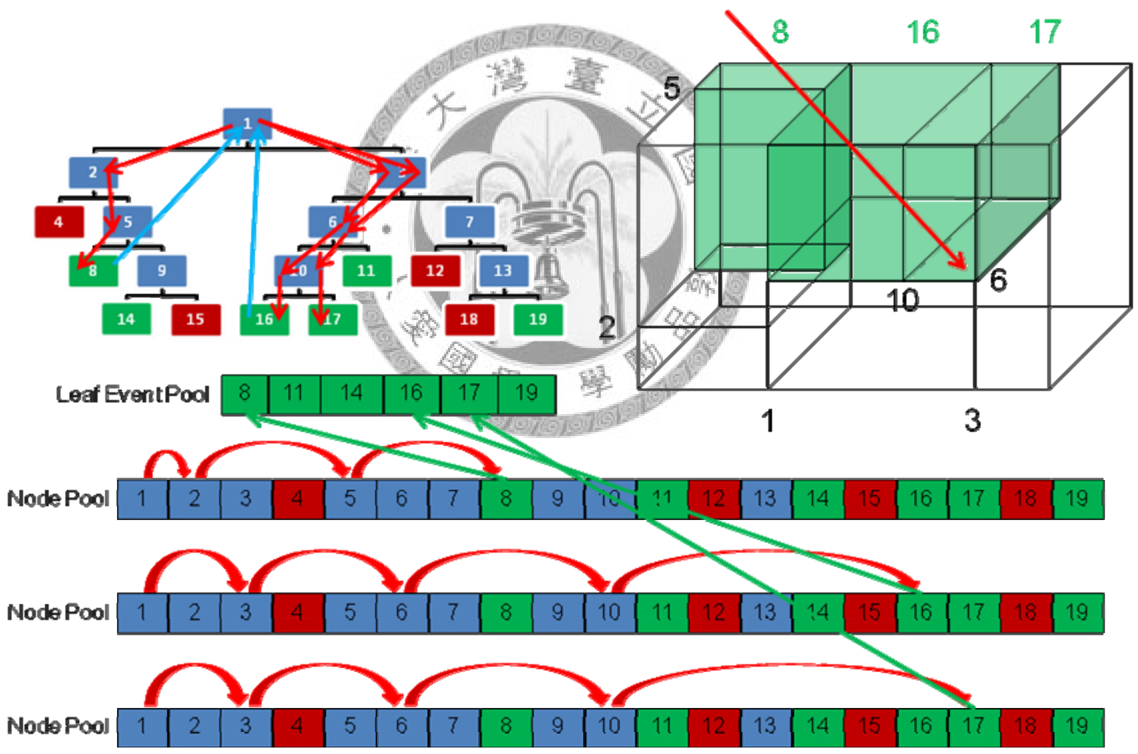

Fig. 6-1 KD-Restart

Although theoretically KD-backtrack may be slightly faster than KD-restart, it consumes much more memory space and may also cause additional burden on the construction stage. The KD-backtrack requires additional information about a pointer to parent and the parent node's AABB (7 floats per node). Thus KD-restart has gradually become recognized as a conventional traversal scheme [13]. Based upon our experiments, KD-restart and KD-backtrack have indistinguishable performance. [7] mentioned that the KD-restart is at most three times slower than the stack based traversal.

6.3 Iterative Single Ray Traversal

For performance reason we implement the traversal as iterative "while loops" rather than tail calls. Here we show our pseudo algorithm of KD-restart implemented as SOA.

```
node = 0;
rayStop = false;
while ( rayStop == false ){
   //Non-leaf node
   if (KD_bLeaf[node] == false){
      if (rayDir[axis] > 0) {
         t_split = (KD_splitPoint[node] - rayStart[axis]) / rayDir[axis];
         if(t_split >= t_max) node = KD_subL[node];
         else if(t_split <= t_min) node = KD_subR[node];
         else {node = KD_subL[node]; t_max = t_split;}
      }
      if (rayDir[axis] < 0) {
         t_split = (KD_splitPoint[node] - rayStart[axis]) / rayDir[axis];
         if(t_split >= t_max) node = KD_subR[node];
         else if(t_split <= t_min) node = KD_subL[node];
         else {node = KD_subR[node]; t_max = t_split;}
      }
      else {
         if(rayStart[axis] < KD_splitPoint[axis]) node = KD_subL[node];        (6.1)
         else if(rayStart[axis] > KD_splitPoint[axis]) node = KD_subR[node];
         else node = KD_subL[node];
      }
   }
   //leaf node
   else {
      if(KD_bEmpty[node] == false) Hit = ray triangle intersection;
      if(Hit) rayStop = true;
      else {
         if(t_max >= t_max_G) rayStop = true;
         else {
            t_min = t_max;
            t_max = t_max_G;
            //Restart
            node = 0;
         }
      }
   }
}                                                                              (6.2)
```

Note that the division by ray direction can be replaced with a precomputed reciprocal.

6.4 Optimized Ray Triangle Intersection

The ray triangle intersection occupies a large fraction of the render time, [33] mentioned that the fraction can be in a range of 75% to 95%.

[5] separated the ray traversal into two phases, the traversal control flow is handled by CPU, and the ray triangle intersection tests are totally moved to GPU.

A conventional routine for the intersection test begins with a distance test, if the distance between the ray origin and the triangle plane is in the interval, then there is a chance to get a hit. The barycentric coordinates are computed to see if the hit point lies inside the triangle [16, 17], note that we store the barycentric coordinates for the afterward shading [30].

$$\begin{aligned}
&P = \alpha A + \beta B + \gamma C = (1 - \beta - \gamma)A + \beta B + \gamma C \\
&P - A = \beta(B - A) + \gamma(C - A) \\
&\mathit{if}\ (0 \le \alpha, \beta, \gamma \le 1)\ \mathit{the\ P\ is\ within\ the\ triangle}
\end{aligned} \tag{6.3}$$

The project method [30] optimizes the barycentric calculation by projecting the triangle and the hit point onto a 2D plane while preserving the barycentric coordinates. The plane is chosen to have the largest projected area for numerical stability.

$$\begin{aligned}
&P_{proj} - A_{proj} = \beta(B_{proj} - A_{proj}) + \gamma(C_{proj} - A_{proj}) \\
&let\ b = C_{proj} - A_{proj}\ and\ c = B_{proj} - A_{proj}\ and\ p = P_{proj} - A_{proj} \\
&p = \beta c + \gamma b \\
&\beta = \frac{bu * pv - bv * pu}{bu * cv - bv * cu}\ and\ \gamma = \frac{cv * pu - cu * pv}{bu * cv - bv * cu}
\end{aligned} \tag{6.4}$$

Note that the projected edges b = (bu, bv) and c = (cu, cv) can be precomputed. The method is almost two times faster than the original [16].

In the same leaf we record the distance of the triangle that has been checked, and if the next triangle has a farther distance it is discarded immediately. Only those with shorter distance have to undergo the barycentric test.

6.5 Hashed Mailboxing

A ray may encounter multiple leaves which contain the same primitives. Mailboxing is applied to record the triangles which have already been tested against the ray, this avoids unnecessary tests. According to [2], a full sized table is impractical. We deploy a similar hashed mailbox. For regular scenes with flat surfaces we did not see any performance gain, but for those with bumps or folds there may be a benefit.

6.6 Parallel Single Ray Traversal on Multi-Core CPU

Since every ray is independent with others during traversal, we can simply distribute the rays to threads and run in parallel. This is also called screen-space parallelization.

Chapter 7 SIMD Incoherent Ray Bundle Tracing

7.1 Data Level Parallelism with Streaming SIMD Extension

The Intel's Streaming SIMD Extension (SSE) was first introduced on Intel's Pentium III, where additional eight 128-bit XMM registers were provided. Four 32-bit floating point values can be packed in one XMM register, and via one instruction we actually operate on four data sets. Versions after SSE2 also support four 32-bit integer values.

The layout of data should be arranged in the structure of array (SOA) to be eligible and beneficial for the SSE implementation.

Hand-written assembly codes are difficult to maintain, furthermore, it loses the support of compiler's rearrangement and optimization, which tightly relates to the problem of data dependency and latency. The SSE intrinsic provides the performance of assembly coding, and also preserves the optimizations from the compiler's view.

7.2 Optimization with SSE Intrinsics

To eliminate the branches induced by if-else clause, a register level macro is applied [2].

```
inline __m128 BLEND4(const __m128 f, const __m128 a, const __m128 b){
  return _mm_or_ps(_mm_and_ps(f, a), _mm_andnot_ps(f, b));          (7.1)
}
```

The reciprocal operation is costly, but is necessary for the inverse of ray direction. A conventional way is to approximate it with a Newton-Raphson iteration [2].

```
inline __m128 RECIPROCAL4(const __m128 a){
  const __m128 rcp =_mm_rcp_ps(a);
  return _mm_sub_ps(_mm_add_ps(rcp, rcp), _mm_mul_ps(_mm_mul_ps(rcp, rcp), a));
}
```

(7.2)

Usually the _mm_movemask_ps is used to check the sign bits of the four ray results, the branch will take place if at least one sign bit is asserted. As mentioned in [24], this operation is expensive and can be replaced by _mm_movemask_epi8.

7.3 The Initial Clipping

Not every ray has a hit with the scene box; these rays are marked as invalid and will not be performed during the traversal. At the very beginning, we have to clip each ray to its valid interval.

```
__m128 t_min4 = _mm_setzero_ps();
__m128 t_max4 = _mm_set_ps1(FLT_MAX);
//-----------------------------------t_min t_max clip on X--------------------------------------
__m128 tClip_min4 = _mm_mul_ps(_mm_sub_ps(_mm_set_ps1(m_min[0]), rayStart4[0]), rayDirR4[0]);
__m128 tClip_max4 = _mm_mul_ps(_mm_sub_ps(_mm_set_ps1(m_max[0]), rayStart4[0]), rayDirR4[0])
__m128 rayDirSign4 = _mm_cmpgt_ps(rayDir4[0], _mm_setzero_ps());
t_min4 = _mm_max_ps(t_min4, BLEND4(rayDirSign4, tClip_min4, tClip_max4));
t_max4 = _mm_min_ps(t_max4, BLEND4(rayDirSign4, tClip_max4, tClip_min4));
//-----------------------------------t_min t_max clip on Y--------------------------------------
tClip_min4 = _mm_mul_ps(_mm_sub_ps(_mm_set_ps1(m_min[1]), rayStart4[1]), rayDirR4[1]);
tClip_max4 = _mm_mul_ps(_mm_sub_ps(_mm_set_ps1(m_max[1]), rayStart4[1]), rayDirR4[1]);
rayDirSign4 = _mm_cmpgt_ps(rayDir4[1], _mm_setzero_ps());
t_min4 = _mm_max_ps(t_min4, BLEND4(rayDirSign4, tClip_min4, tClip_max4));
t_max4 = _mm_min_ps(t_max4, BLEND4(rayDirSign4, tClip_max4, tClip_min4));
//-----------------------------------t_min t_max clip on Z--------------------------------------
tClip_min4 = _mm_mul_ps(_mm_sub_ps(_mm_set_ps1(m_min[2]), rayStart4[2]), rayDirR4[2]);
tClip_max4 = _mm_mul_ps(_mm_sub_ps(_mm_set_ps1(m_max[2]), rayStart4[2]), rayDirR4[2]);
rayDirSign4 = _mm_cmpgt_ps(rayDir4[2], _mm_setzero_ps());
t_min4 = _mm_max_ps(t_min4, BLEND4(rayDirSign4, tClip_min4, tClip_max4));
t_max4 = _mm_min_ps(t_max4, BLEND4(rayDirSign4, tClip_max4, tClip_min4));
//-----------------------------------Clip the rayLength-----------------------------------------
t_max4 = _mm_min_ps(t_max4, rayLength4);
//-----------------------------------Check the intersection-------------------------------------
bIntersection4 = _mm_cmple_ps(t_min4, t_max4);
```

(7.3)

7.4 SIMD Ray Triangle Intersection

There are two ways to do this [30]. First we can consider intersecting one ray with four triangles. Obviously there is some problem with this; not every leaf has a multiple of four triangles, and usually they have only one or two triangles. Also KD tree tends to perform better with small leaves [31].

The alternative is to test four rays against one triangle. This makes sense because rays in a bundle are from consecutive pixels, and usually have similar origins and directions. There is much of a chance to have all four rays collided on one big triangle.

7.5 Omnidirectional Ray Traversal for KD Tree

The traditional SSE traversal requires that the ray bundle is coherent in direction, that is, the four rays have the same signs in all three dimensions. Early exit is favored, because the nodes traversed are in the ascending distance order from all four ray's origins. On the contrary, the need to classify the rays into coherent group and treat them individually inevitably lowers the utilization of the SIMD fashion. An alternative way is to cluster the rays into eight coherent groups, but it results in bad work sharing on multi-core architecture.

Omnidirectional traversal [24] is devised to process incoherent ray bundles. Compared with the coherent traversal, it greatly reduces the number of triangle intersection tests and reports an average of 1.5X speedup [24]. However, it comes at the expense of no early exit. We cannot ensure that either the left child or the right child is traversed first for incoherent rays; the only thing we consider is whether both children are traversed or not.

```
const __m128 mix0f = _mm_castsi128_ps(_mm_set1_epi32(0x0000ffff));
__m128 rayTracing4 = _mm_and_ps(_mm_castsi128_ps(_mm_set1_epi32(0xffffffff)), rayValid4);

while(_mm_movemask_ps(rayTracing4)){
   if(kdg_bLeaf[node] == false){
      DWORD axis = kdg_splitAxis[node];
      __m128 timeHitSplit4 = _mm_mul_ps(
                  _mm_sub_ps(_mm_set_ps1(kdg_splitPoint[node]), rayStart4[axis]), rayDirR4[axis]);
      __m128 maskDir4 = _mm_cmplt_ps(rayDir4[axis], _mm_setzero_ps());
      __m128 maskNear4 = _mm_cmple_ps(t_min4, timeHitSplit4);
      __m128 maskFar4 = _mm_cmpge_ps(t_max4, timeHitSplit4);
      __m128 maskSelect4 = _mm_xor_ps(mix0f, maskDir4);
      __m128 maskValid4 = _mm_cmple_ps(t_min4, t_max4);
      __m128 maskHit4 = _mm_and_ps(maskValid4, BLEND4(maskSelect4, maskNear4, maskFar4));
      int hit4 = _mm_movemask_epi8(_mm_castps_si128(maskHit4));
      int hitRight4 = hit4 & 0xcccc;
      int hitLeft4 = hit4 & 0x3333;
      if(hitLeft4 == 0){node = kdg_subR[node];continue;}
      if(hitRight4 == 0){node = kdg_subL[node];continue;}
      PUSH(kdg_subR[node],
         BLEND4(maskDir4, t_min4, _mm_max_ps(timeHitSplit4, t_min4)),
         BLEND4(maskDir4, _mm_min_ps(timeHitSplit4, t_max4), t_max4));
      node = kdg_subL[node];
      t_min4 = BLEND4(maskDir4, _mm_max_ps(timeHitSplit4, t_min4), t_min4);
      t_max4 = BLEND4(maskDir4, t_max4, _mm_min_ps(timeHitSplit4, t_max4));
   }
   else{
      if(kdg_bEmpty[node] == false){
         DO TRIANGLE INTERSECTION HERE
      }
      if(nodeStack)POP(node, t_min4, t_max4);
      else rayTracing4 = _mm_setzero_ps();
   }
}
```

(7.4)

The trick is to select the near child and the far child by the ray direction. For rays with positive directions [far, near] is recorded, for those with negative directions [near, far] is recorded instead. Now we have [right, left] for all four rays, and we can ignore the right child if all rays go to the left.

Note that there is no early exit; some rays are traversed in the reversed order. An intersection with triangle is valid only if the hit time is smaller than the one before. And the barycentric test is performed only if at least one ray has a valid hit time.

Though theoretically the SIMD implementation brings 4X speedup over the single ray traversal, in regular conditions it reports a 1.5X to 2.5X speedup [3, 4]. Due to some lack of optimizations our implementation is just slightly faster than the single ray traversal.

Chapter 8 Parallel Primitives on GPU

8.1 Bitonic Merge Sort

Bitonic merge sort [1, 22] is a commonly used divide-and-conquer algorithm on GPU. The concept of bitonic merge is to merge an equal-sized ascending and descending sequence into one ascending or descending sequence.

A mapping of bitonic merge to CUDA can be done in two levels. It begins with small chunk merges done within individual blocks. And then large chunk merge is applied every time we double the merge size.

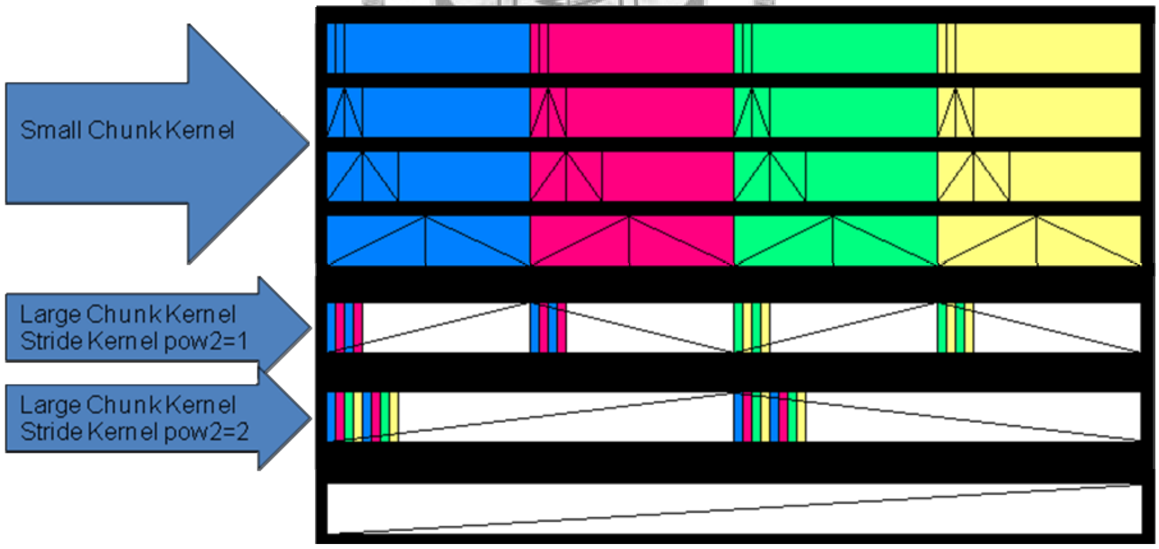

Fig. 8-1 A bitonic merge sort of 2048 elements on CUDA, with block size = 512

8.2 Prefix Sum (scan)

Although modern GPUs become more powerful and general purpose, not all algorithms can be easily mapped to GPU. Problems like scan, split, and sorting, demand “global knowledge” of the input data. They suit far well to serial processors as Intel x86, and porting them to GPU requires different implementation. The prefix-sum (scan) [10, 26] is one of the fundamental algorithms, it is also the primitive operation of many advanced applications.

The scan consists of two phases: reduction (up-sweep) and down-sweep.

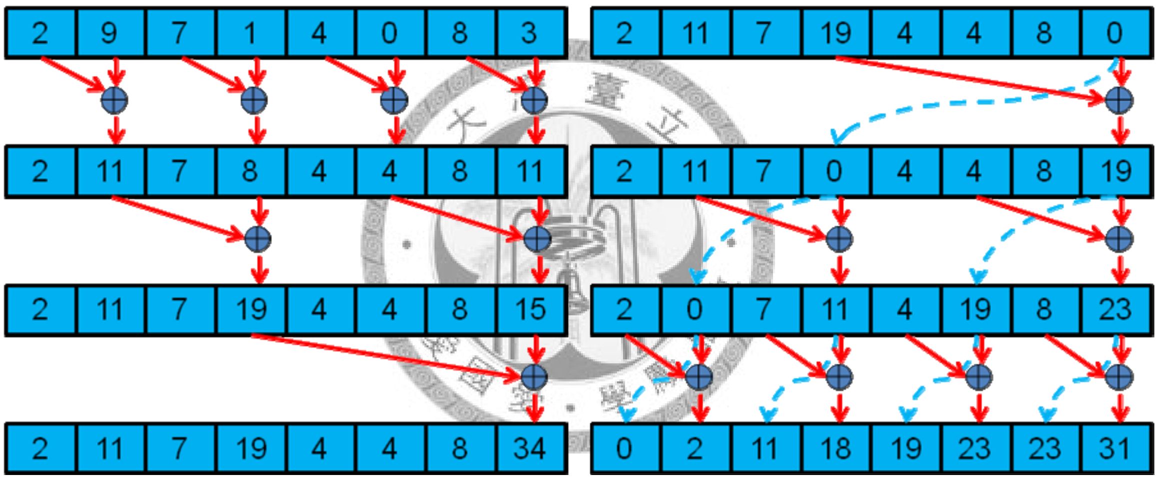

Fig. 8-2 Unsegmented scan: reduction (left) and down-sweep (right)

8.3 Segmented Prefix Sum (scan)

When the algorithm has to be applied to different sections of the array individually, the segmented version is used. A head flag array of the same length with the input data is needed to indicate the position of a new segment.

$$\begin{array}{lcccccccccccccc} \textit{Data} & 5 & 8 & 2 & 4 & 0 & 9 & 1 & 7 & 3 & 8 & 2 & 5 & 4 & 1 \\ \textit{Flag} & 1 & 0 & 0 & 0 & 0 & 0 & 0 & 1 & 0 & 0 & 0 & 1 & 0 & 0 \\ \textit{Out} & 0 & 5 & 13 & 15 & 19 & 19 & 28 & 0 & 7 & 10 & 18 & 0 & 5 & 9 \end{array} \qquad (8.1)$$

The pseudo algorithm is as follows.

```
Reduction
for $d = 0$ to $\log_2 n - 1$ do
    for all $k = 0$ to $n - 1$ by $2^{d+1}$ in parallel do
        if $f[k + 2^{d+1} - 1]$ is not set then
            $x[k + 2^{d+1} - 1] \leftarrow x[k + 2^d - 1] + x[k + 2^{d+1} - 1]$
        $f[k + 2^{d+1} - 1] \leftarrow f[k + 2^d - 1] \mid f[k + 2^{d+1} - 1]$
                                                                    (8.2)
```

```
Down sweep
$x[n - 1] \leftarrow 0$
for $d = \log_2 n - 1$ down to $0$ do
    for all $k = 0$ to $n - 1$ by $2^{d+1}$ in parallel do
        $t \leftarrow x[k + 2^d - 1]$
        $x[k + 2^d - 1] \leftarrow x[k + 2^{d+1} - 1]$
        if $f_{original}[k + 2^d]$ is set then
            $x[k + 2^{d+1} - 1] \leftarrow 0$
        else if $f[k + 2^d - 1]$ is set then
            $x[k + 2^{d+1} - 1] \leftarrow t$
        else
            $x[k + 2^{d+1} - 1] \leftarrow t + x[k + 2^{d+1} - 1]$
        unset $f[k + 2^d - 1]$
                                                                    (8.3)
```

8.4 Segmented Split

The split operation divides a vector of true/false values into two parts, with the first filled with all false values, and the other with all true values. The segmented split factors the operation into sections of the input. Note that it is based on the segmented scan.

Chapter 9 Experiments and Results

9.1 Ray Traced Scenes

Here we show the scenes of 800x800 resolution rendered with one primary ray, one shadow ray and one point light source. The model is placed in a textured box.

The program was done in C++, and openMP for the parallel implementations. Images were presented onto screen using WinGDI.

All the performance measurements were from a WindowsXP desktop, with Intel Core2 Quad 9550 (2.83Ghz), NVIDIA GTX 260+.

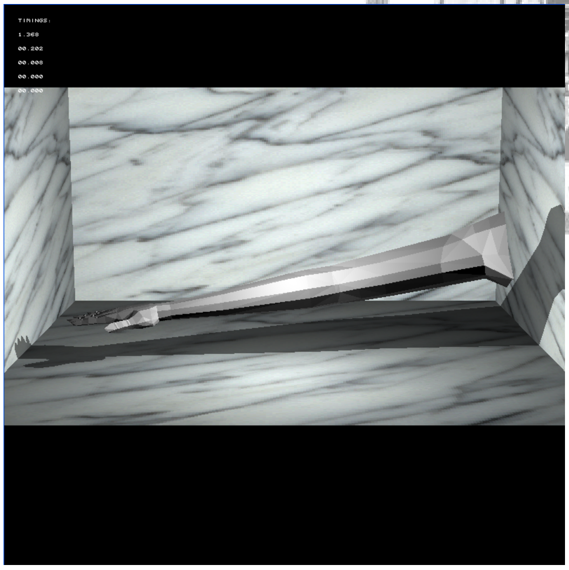

```
TIMINGS:
1.368
00.202
00.008
00.000
00.000
```

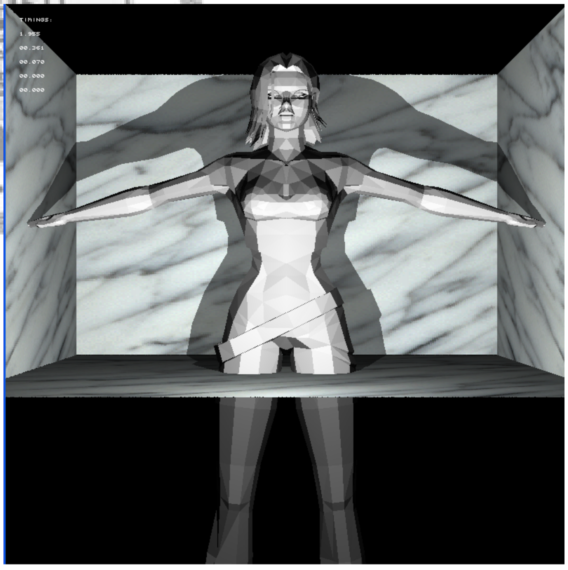

```
TIMINGS:
1.955
00.361
00.070
00.000
00.000
```

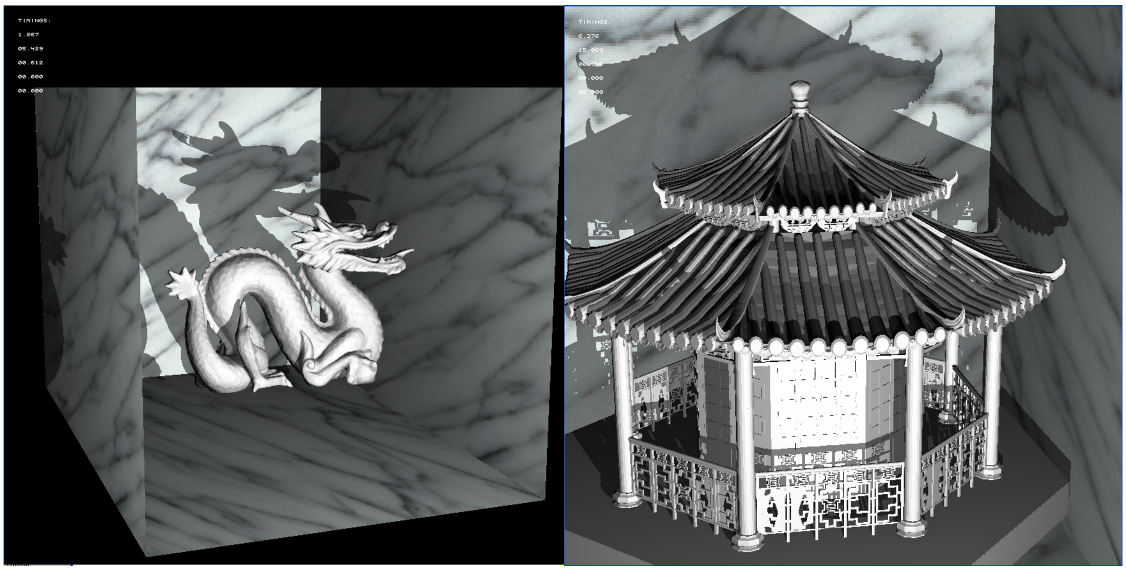

Fig. 9-1 (a) Arm, 816 triangles (b) Kila, 4,110 triangles (c) Dragon, 65,533 triangles (d) Temple, 222,900 triangles

9.2 Serial Domain Partitioning

In chapter 4 we have presented the subtree construction in parallel, but with domain partitioning in serial. The benchmark is as below.

Table 9-1 Construction time (sec) with subtree construction in parallel

# Threads	#Sub(partition)	Arm	Kila	Dragon	Temple
1	1	0.011	0.054	0.807	2.902
2	2	0.008	0.034	0.504	1.727
4	4	0.006	0.024	0.369	1.254
4	8	0.006	0.024	0.365	1.254

The construction has far better scalability for large models. Anyway, the scalability is sub linear with number of threads.

9.3 Parallel Domain Partitioning with 1D Binning

We replace the serial domain partitioning with a parallel 1D binning, making the construction process achieve a higher scalability.

Table 9-2 Construction time (sec) with parallel subtree construction and parallel 1D binning

# Threads	#Sub(partition)	Arm	Kila	Dragon	Temple
1	1	0.011	0.056	0.822	2.887
2	2	0.008	0.030	0.459	1.552
4	4	0.006	0.019	0.271	0.923
4	8	0.005	0.019	0.266	0.901

The scalability is way better than the one with serial domain partitioning, achieves more than 3X speedup for large models. For a finer partitioning, there is a slight gain since the O(NlogN) merge sort is divided into smaller pieces. Also we wonder that in a finer partitioned scene the workload is better balanced among the threads.

9.4 Parallel Domain Partitioning with 3D Binning

Compared to 1D binning, the 3D binning costs more time in the construction stage, but generates better partitions.

Table 9-3 Construction time (sec) with parallel subtree construction and parallel 3D binning

# Threads	#Sub(partition)	Arm	Kila	Dragon	Temple
1	1	0.012	0.053	0.792	2.804
2	2	0.009	0.040	0.611	2.112
4	4	0.008	0.032	0.466	1.688
4	8	0.008	0.033	0.491	1.697

Maybe due to some implementation problem, the 3D binning is considerably slower than the 1D binning.

9.5 Render Time and the Quality of Tree

We apply openMP to parallelize the optimized single ray traversal, and benchmark render time with the different construction scheme. All scenes are rendered with all 4 cores, what we want to see is the effect of different partitioning scheme on the quality of tree.

Table 9-4 Render time (4 threads) (sec) with subtree construction in parallel

# Threads	#Sub(partition)	Arm	Kila	Dragon	Temple
1	1	0.659	0.877	0.982	6.538
2	2	0.646	0.910	0.987	6.473

4	4	0.645	0.941	1.029	6.437
4	8	0.654	0.891	1.081	6.443

Since the partitioning is done in 3D, we preserve the quality of the tree even with a large number of partitions.

Table 9-5 Render time (4 threads) (sec) with parallel subtree construction and parallel 1D binning

# Threads	#Sub(partition)	Arm	Kila	Dragon	Temple
1	1	0.651	0.875	0.977	6.535
2	2	0.636	0.931	0.992	6.410
4	4	0.648	0.929	1.072	6.381
4	8	0.717	0.919	1.267	6.652

We wonder that in a finer partitioned scene the 1D binning hurts the quality of the tree; the performance of traversal has an obvious decline with a partition of 8.

Table 9-6 Render time (4 threads) (sec) with parallel subtree construction and parallel 3D binning

# Threads	#Sub(partition)	Arm	Kila	Dragon	Temple
1	1	0.646	0.887	0.991	6.507
2	2	0.639	0.909	1.009	6.363

4	4	0.659	0.923	1.036	6.453
4	8	0.694	0.934	1.119	6.409

In a partition of 8, the 3D binning renders slightly faster than the 1D binning, but still cannot make up for the cost at the construction stage.

Chapter 10 Conclusions and Future Work

10.1 Conclusions

We have succeeded in achieving a high scalability of parallel KD tree construction on the shared memory based multi-core CPU. The work load is well balanced among all the threads, and the quality loss is in a limited range. The program can be ported to various CPUs with different number of cores. Our algorithm may benefit many interactive applications. In near future ray traced games with similar algorithms will be available on everyone's desktop.

10.2 Future Work

We would like to look for the ways to simplify and speedup some operations in the KD tree construction. And we are going to figure out some more efficient approaches for animated scenes; instead of reconstruction from scratch every frame, for structured scenes some partial updates of the tree may be enough.

Also the coherent ray bundle traversal and the data level parallelism with Intel SSE are the crucial issues. Our future modifications will focus on exploiting the coherent problems.

Reference

1. Batcher, K., Sorting networks and their applications. in, (1968), ACM New York, NY, USA, 307-314.
2. Benthin, C. Realtime Ray Tracing on Current CPU Architectures, Universitatsbibliothek, 2006.
3. Boulos, S., Edwards, D., Lacewell, J., Kniss, J., Kautz, J., Shirley, P. and Wald, I., Packet-based whitted and distribution ray tracing. in *Proceedings of Graphics Interface*, (2007), ACM New York, NY, USA, 177-184.
4. Boulos, S., Wald, I. and Benthin, C., Adaptive ray packet reordering. in *IEEE Symposium on Interactive Ray Tracing*
(2008), 131-138.
5. Carr, N., Hall, J. and Hart, J., The ray engine. in *Proceedings of the ACM SIGGRAPH/EUROGRAPHICS conference on Graphics hardware*, (2002), Eurographics Association Aire-la-Ville, Switzerland, Switzerland, 37-46.
6. Chapman, B., Jost, G., Van Der Pas, R. and Kuck, D. *Using OpenMP: portable shared memory parallel programming*. The MIT Press, 2007.
7. Foley, T. and Sugerman, J., KD-tree acceleration structures for a GPU raytracer. in *Proceedings of the ACM SIGGRAPH/EUROGRAPHICS conference on Graphics hardware*, (2005).
8. Gottschalk, S., Lin, M. and Manocha, D., OBBTree: A hierarchical structure for rapid interference detection. in *ACM Transactions on Graphics ACM SIGGRAPH*, (1996), ACM New York, NY, USA, 171-180.
9. Gunther, J., Friedrich, H., Seidel, H. and Slusallek, P. Interactive ray tracing of skinned animations. *The Visual Computer*, *22* (9). 785-792.
10. Harris, M., Sengupta, S. and Owens, J. Parallel prefix sum (scan) with CUDA. *GPU Gems*, *3*.
11. Havran, V. Heuristic ray shooting algorithms *Unpublished doctoral dissertation, Czech Technical University in Prague*, 2000.
12. Havran, V., Herzog, R. and Seidel, H., On the fast construction of spatial hierarchies for ray tracing. in *IEEE Symposium on Interactive*

Ray Tracing, (2006), 71-80.

13. Horn, D., Sugerman, J., Houston, M. and Hanrahan, P., Interactive kd tree GPU raytracing. in *ACM SIGGRAPH symposium on Interactive 3D graphics and games*, (2007), ACM New York, NY, USA, 167-174.
14. Hunt, W., Mark, W. and Stoll, G., Fast kd-tree construction with an adaptive error-bounded heuristic. in *IEEE Symposium on Interactive Ray Tracing*, (2006), 81-88.
15. MacDonald, J. and Booth, K. Heuristics for ray tracing using space subdivision. *The Visual Computer*, *6* (3). 153-166.
16. Moller, T. A fast triangle-triangle intersection test. *Journal of graphics tools*, *2* (2). 25-30.
17. Moller, T. and Trumbore, B. Fast, minimum storage ray-triangle intersection. *Graphics Tools: The Jgt Editors' Choice*. 181.
18. Pharr, M. and Humphreys, G. *Physically Based Rendering: From Theory to Implementation*. Morgan Kaufmann, 2004.
19. Popov, S., Gunther, J., Seidel, H. and Slusallek, P., Experiences with streaming construction of SAH KD-trees. in *IEEE Symposium on Interactive Ray Tracing*, (2006), 89-94.
20. Popov, S., Gunther, J., Seidel, H. and Slusallek, P., Stackless kd-tree traversal for high performance GPU ray tracing. in *Eurographics*, (2007), Blackwell Publishing Ltd, 415-424.
21. Purcell, T., Buck, I., Mark, W. and Hanrahan, P., Ray tracing on programmable graphics hardware. in *International Conference on Computer Graphics and Interactive Techniques*, (2005), ACM New York, NY, USA.
22. Purcell, T., Donner, C., Cammarano, M., Jensen, H. and Hanrahan, P., Photon mapping on programmable graphics hardware. in *Proceedings of the ACM SIGGRAPH/EUROGRAPHICS conference on Graphics hardware*

(2003), Eurographics Association Aire-la-Ville, Switzerland, Switzerland, 41-50.

23. Quinn, M. *Parallel Programming in C with MPI and OpenMP*, 2004.
24. Reshetov, A., Omnidirectional ray tracing traversal algorithm for kd-trees. in *IEEE Symposium on Interactive Ray Tracing*, (2006), 57-60.
25. Reshetov, A., Soupikov, A. and Hurley, J. Multi-level ray tracing

algorithm. *Proceedings of ACM SIGGRAPH 2005*, *24* (3). 1176-1185.

26. Sengupta, S., Harris, M., Zhang, Y. and Owens, J., Scan primitives for GPU computing. in *Proceedings of the ACM SIGGRAPH/EUROGRAPHICS conference on Graphics hardware*, (2007), Eurographics Association Aire-la-Ville, Switzerland, Switzerland, 97-106.
27. Shevtsov, M., Soupikov, A. and Kapustin, A., Highly parallel fast kd-tree construction for interactive ray tracing of dynamic scenes. in *Eurographics*, (2007), 395-404.
28. Stoll, G. Part II: Achieving real time-optimization techniques. *SIGGRAPH 2005 Course on Interactive Ray Tracing*.
29. Wachter, C. and Keller, A. Instant ray tracing: The bounding interval hierarchy. *Rendering techniques*, *2006*. 139-149.
30. Wald, I. Realtime ray tracing and interactive global illumination, Universitatsbibliothek, 2004.
31. Wald, I., Benthin, C. and Boulos, S., Getting rid of packets-Efficient SIMD single-ray traversal using multi-branching BVHs. in *IEEE Symposium on Interactive Ray Tracing*, (2008), 49-57.
32. Wald, I. and Havran, V., On building fast kd-trees for ray tracing, and on doing that in O (N log N). in *IEEE Symposium on Interactive Ray Tracing*, (2006), 61-69.
33. Whitted, T. An improved illumination model for shaded display. *ACM Communications*.
34. Woop, S., Marmitt, G. and Slusallek, P. B-kd trees for hardware accelerated ray tracing of dynamic scenes. *Graphics Hardware 2006: Eurographics Suymposium Procceding Vienna, Austria September 3-4, 2006*. 67.